

“New Directions in Low-Dimensional Electron Systems”,  
KITP, UCSB, February 23-27, 2009

# Entanglement Spectrum of Quantum Hall States

F. D.M. Haldane, Princeton University

- ★ Observing Topological Order using entanglement
- ★ The “entanglement spectrum” gives more information than the von Neumann entropy:
- ★ FQHE model states, cft, Jack polynomials, and the “entanglement gap”

(Pre-Jack-polynomial results first reported at:  
QCMBS conference, Feb 2006)

[http://www.qcmbs.org/documents/prompt/HaldaneFDM\\_20060201.pdf](http://www.qcmbs.org/documents/prompt/HaldaneFDM_20060201.pdf)

Jack polynomial connection:

- Feigin et al. 2002 (arXiv:math/0112127)
- Bernevig and FDMH, PRL 100, 246802 (2008)

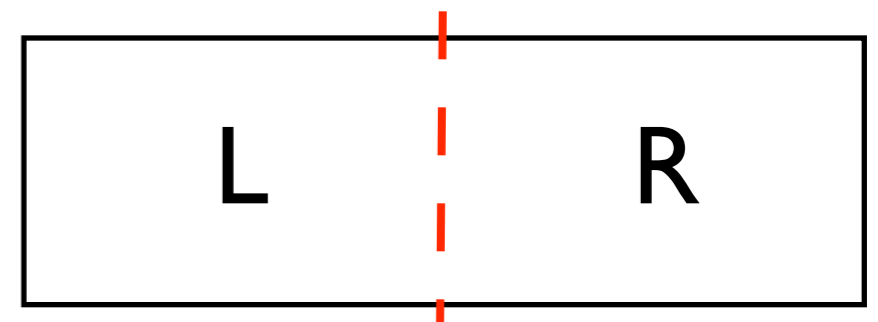
Entanglement spectrum:

- Li and FDMH, PRL 101, 010504 (2008)

# Bipartite entanglement of (pure) quantum states

$$|\Psi\rangle = \sum_{\alpha=1}^{N_L} \sum_{\beta=1}^{N_R} W_{\alpha\beta} |\phi_{\alpha}^L\rangle \otimes |\phi_{\beta}^R\rangle$$

$$\langle \phi_{\alpha}^L | \phi_{\alpha'}^L \rangle \langle \phi_{\beta}^R | \phi_{\beta'}^R \rangle = \delta_{\alpha\alpha'} \delta_{\beta\beta'}$$



- Spatial decomposition of wavefunction into two parts
- Singular value (Schmidt) decomposition of  $W$ :

$$W_{\alpha\beta} = \sum_{\lambda=1}^{N_0} e^{-\frac{1}{2}\xi_{\lambda}} u_{\alpha\lambda}^L u_{\beta\lambda}^R$$

$$\sum_{\alpha} (u_{\alpha\lambda}^L)^* u_{\alpha\lambda'} = \sum_{\beta} (u_{\beta\lambda}^R)^* u_{\beta\lambda'} = \delta_{\lambda\lambda'}$$

$$N_0 \leq N_L, N_R$$

**Schmidt eigenvalues**  
(real positive)

$$\langle \Psi | \Psi \rangle = \sum_{\lambda} e^{-\frac{1}{2}\xi_{\lambda}}$$

(don't care if normalized or not)

# Von Neuman (bipartite) entanglement entropy:

$$S_{VN} = - \sum_{\lambda} p_{\lambda} \ln p_{\lambda} \quad \sum_{\lambda} p_{\lambda} = 1$$

$$p_{\lambda} = \frac{e^{-\xi_{\lambda}}}{Z}$$

$$Z = \sum_{\lambda} e^{-\xi_{\lambda}}$$

dimensionless analog of  
“energy levels”

- generalize this to

$$S_{VN} = S(1),$$

$$S(\beta) = - \sum_{\lambda} p_{\lambda}(\beta) \ln p_{\lambda}(\beta)$$

$$P_{\lambda}(\beta) = \frac{e^{-\beta \xi_{\lambda}}}{Z(\beta)}$$

$$Z(\beta) = \sum_{\lambda} e^{-\beta \xi_{\lambda}}$$

dimensionless analog of  
“inverse temperature”

1D system (strip, embedded in infinite system)



$\lim_{\ell \rightarrow \infty} S_{VN} \rightarrow \text{constant}$  (ground state of gapped, non-critical system)

$\lim_{\ell \rightarrow \infty} S_{VN} \rightarrow \frac{1}{3} c \ln(\ell/a)$  (ground state of gapless critical system)

**conformal anomaly**

- Lots of recent interest in Von-Neumann entanglement entropy of Condensed matter ground states probably due to this famous result

generalization:  $\lim_{\ell \rightarrow \infty} S(\beta) \rightarrow \frac{\beta^{-1}}{3} c \ln(\ell/a)$  (Linear in “temperature”)

- Rather than just representing entanglement by a single number  $S_{VN}$ , it is useful to examine the full “entanglement spectrum”  $\xi_\lambda$
- In particular, examine its “low-energy” structure (or examine  $S(\beta)$  for large  $\beta$  (low “temperature” limit))

result: gapped systems with topological order appear to always have a gapless entanglement spectrum

# Classification of Schmidt entanglement states:

- If the state is a singlet representation of some group, the entanglement eigenstates form irreducible representations.

example: spin-singlet state

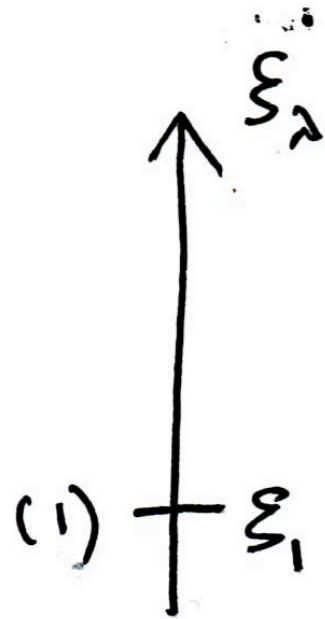
$$|\Psi_{S=0}\rangle = \sum_{S,\lambda} e^{-\frac{1}{2}\xi_{S\lambda}} \sum_{M=-S}^S (-1)^{S-M} |\Psi_{S,M\lambda}^L\rangle \otimes |\Psi_{S,-M\lambda}^R\rangle$$

entanglement spectrum has spin multiplets

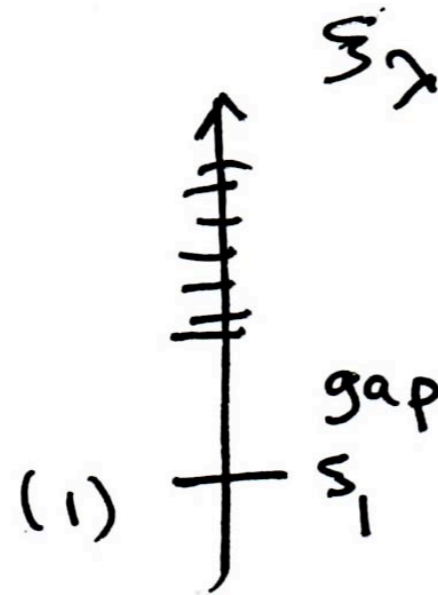
# Example: $S=1$ chain

entanglement spectrum "ground state" is a degenerate  $S=1/2$  doublet in the topologically-ordered "Haldane gap" phase

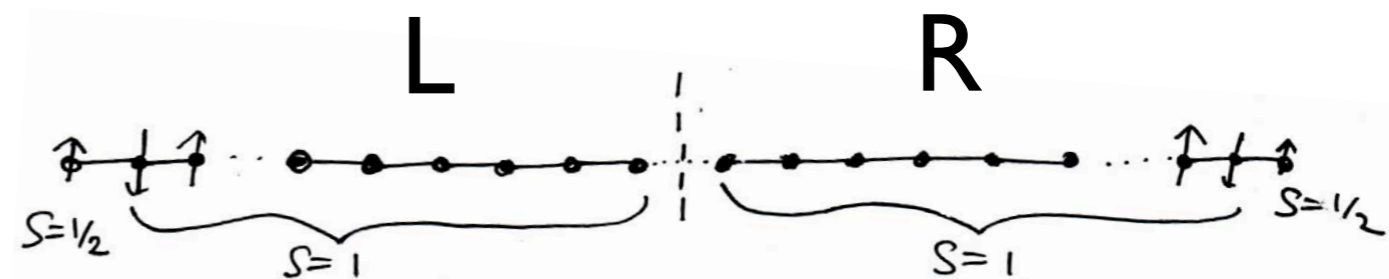
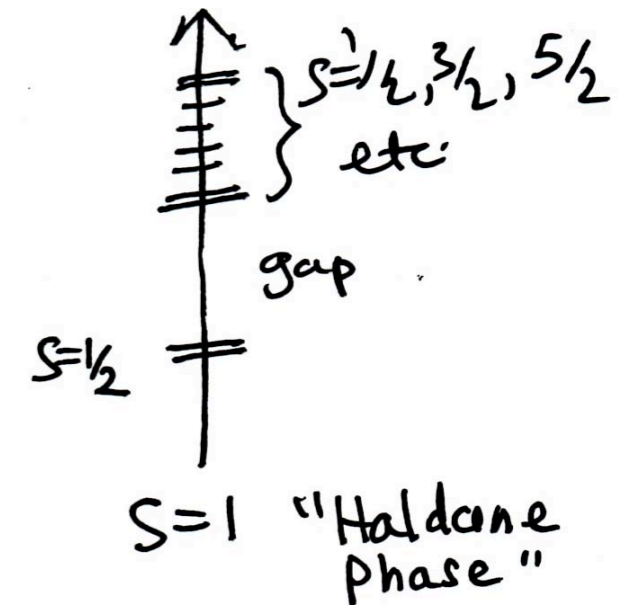
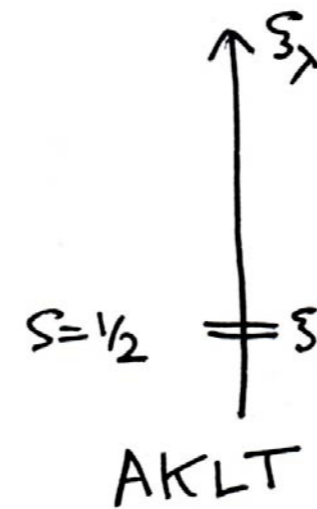
## No topological order



simple product state



not a simple product state, but still a generic topologically-trivial state.



Note that the low "energy"  $S=1/2$  entanglement degrees of freedom become the free  $S=1/2$  edge state if a physical cut is made!



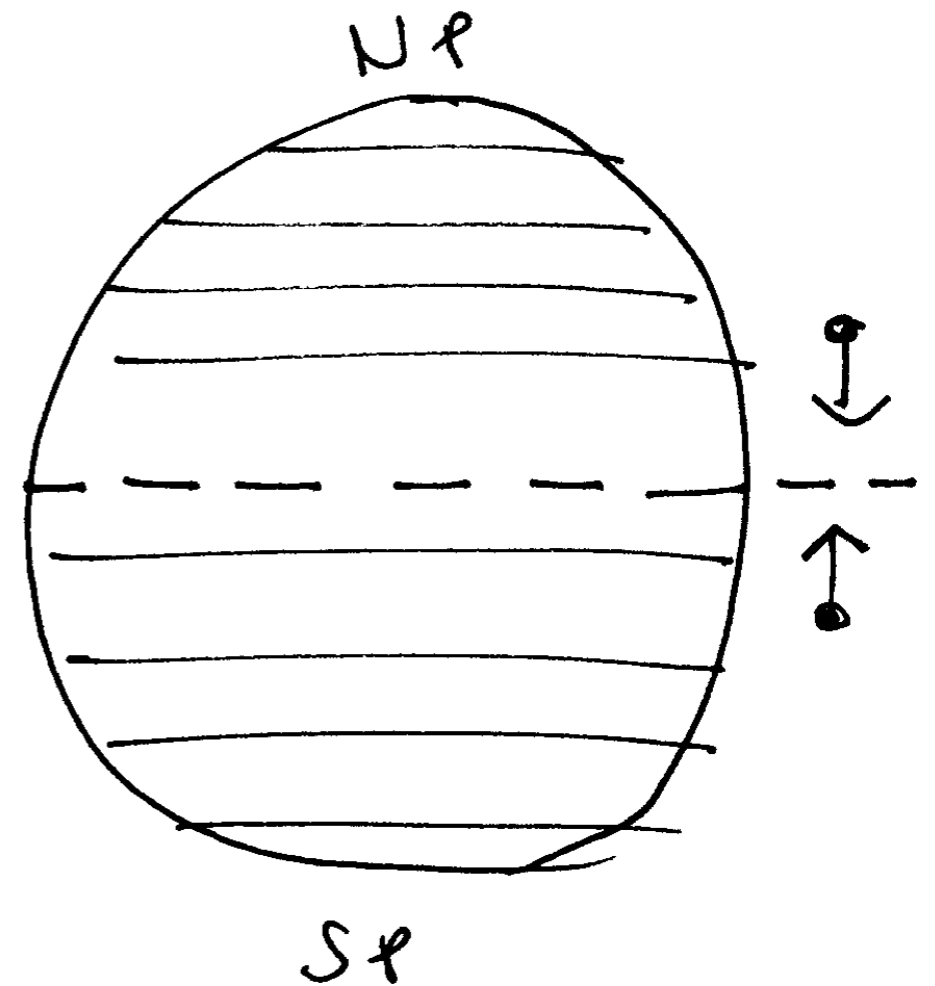
- Divide a translationally-invariant gapped infinite  $d$ -dimensional system into two semi-infinite pieces along a  $(d-1)$ -dimensional translationally-invariant plane.
- Can classify entanglement spectrum by  $(d-1)$ -dimensional momentum or Bloch vector parallel to boundary.

# second example: FQHE states:

- Edges of gapped bulk FQHE states are described by conformal field theories.
- Expect that the low-energy entanglement spectrum is the same (gapless) cft. (Correct!)
- Analogs of AKLT state are the model wavefunctions (Laughlin, Moore-Read, etc) that are exact ground states of “special” models. They have a simpler entanglement spectrum than “generic” states with the same topological order.

# FQHE states in spherical geometry

- Schmidt decomposition of Fock space into N and S hemispheres.
- Classify states by  $L_z$  and  $N_e$  in northern hemisphere, relative to dominant configuration.



FQHE states have  $L=0$

# Represent bipartite Schmidt decomposition like an excitation spectrum

Hui Li and FDMH,  
PRL **101**,010504 (2008)

$$|\Psi\rangle = \sum_{\alpha} e^{-\beta_{\alpha}/2} |\Psi_{N\alpha}\rangle \otimes |\Psi_{S\alpha}\rangle$$

- like CFT of edge states.
- A lot more information than single number (entropy)
- many zero eigenvalues (infinite “pseudoenergies”)

$$e^{-\beta_{\alpha}} = 0$$

(due to “squeezing” (dominance) property of Laughlin wavefunction)

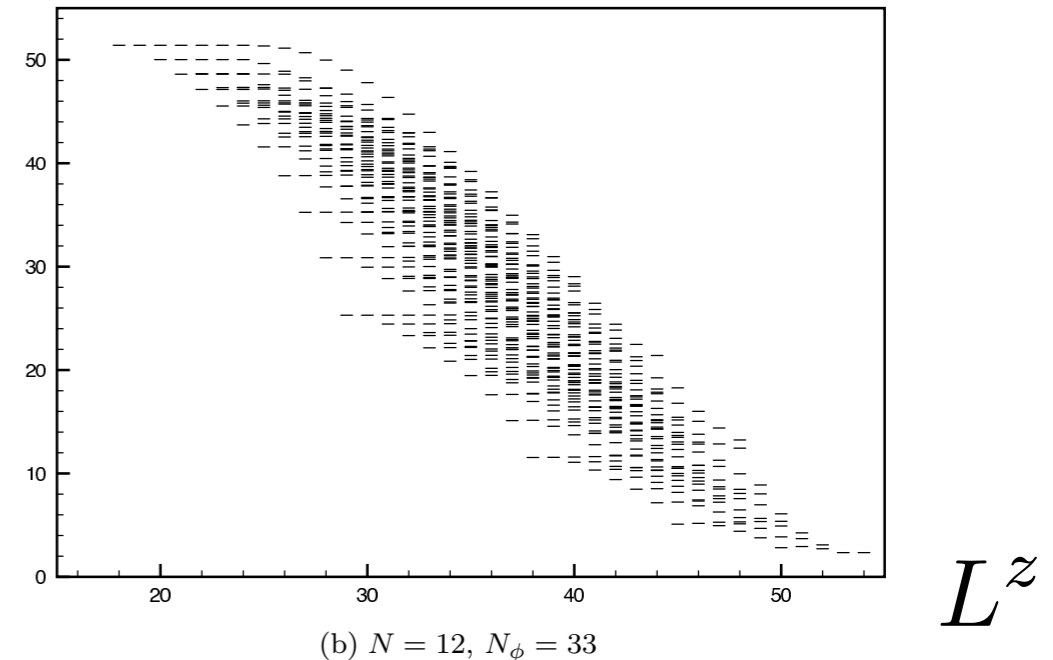
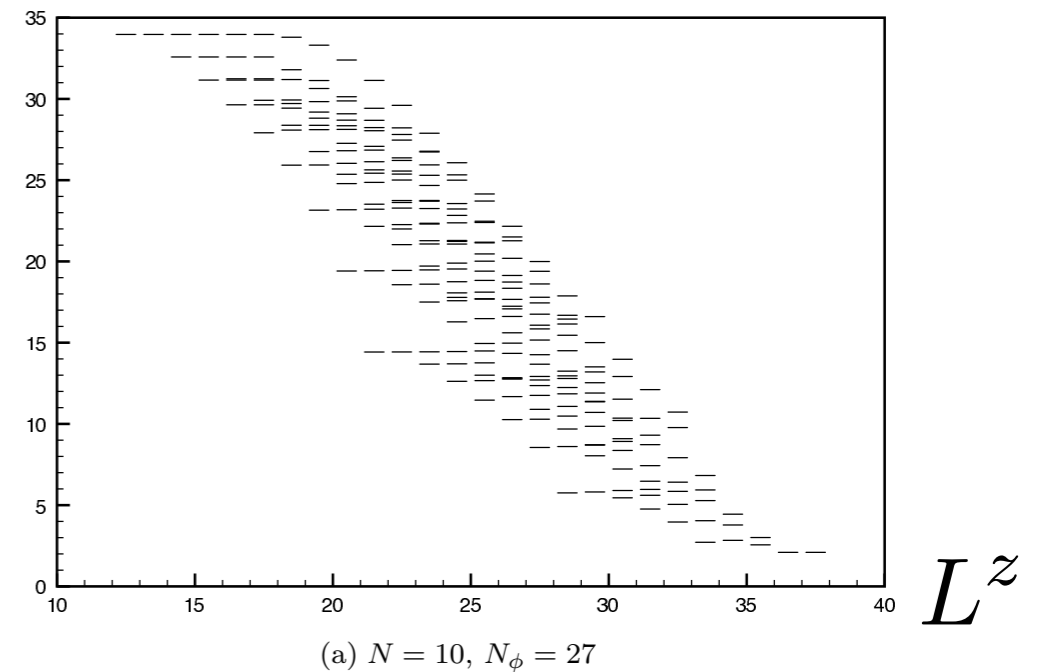


FIG. 1: Entanglement spectrum for the 1/3-filling Laughlin states, for  $N = 10, m = 3, N_{\phi} = 27$  and  $N = 12, m = 3, N_{\phi} = 33$ . Only sectors of  $N_A = N_B = N/2$  are shown.

This special structure is a property of cft-based  
“model” wavefunctions such as Laughlin,  
Moore-Read, Read-Rezayi, etc.

- These wavefunctions are homogenous polynomials with a “dominance” property

$$\psi = f(z_1, z_2, \dots, z_N) \psi_0$$

**polynomial (Gaussian)**

$$f(z_1, z_2, \dots, z_N) = \sum_{\{m_i\}} A(\{m_i\}) \prod_i z_i^{m_i}$$

$$n_m = \sum_i \delta_{m, m_i}, \quad m = 0, 1, \dots$$

**“occupation numbers”  
(of “orbitals”  $z^m$ )**

$$A(\{m_i\}) \equiv A(\{n_m\}) = 0, \text{ unless } \{n_m\} \preceq \{n_m^0\}$$

**dominance**

**“root occupation configuration”**

- “dominated by” = “can be obtained by squeezing”

$$(z_1 - z_2)^3 = (z_1^3 z_2^0 - z_2^3 z_1^0) - 3(z_1^2 z_2^1 - z_2^2 z_1^1)$$

occupations: 100|000...  $\succ$  01|0000...

01|0000...

squeeze

squeezing conserves

$$M = \sum_i m_i = \sum_m m n_m$$

100|000... is the “root” configuration

- The root has the maximum variance

$$V = \sum_{i < j} (m_i - m_j)^2 = \sum_{m < m'} (m - m')^2 n_m n_{m'}$$

The only configurations present in the wavefunction in addition to the root are those dominated by (squeezable from) the root

$$(z_1 - z_2)^3 = (z_1 - z_2) J_{\{\bar{m}\}}^{-2}(z_1, z_2)$$

Jack (symmetric) polynomial

$$J^\alpha(\{z_i\}), \quad \alpha = -2$$

bosonic root, related to 100|...

- 1/3 Laughlin has root  $1001001001001001..$
- 1/3 Laughlin state with quasiholes spanned by vandermonde times  $\alpha = -2$  Jack states with roots like  $10010\underbrace{0}_\bullet 10010010\underbrace{0}_\bullet 1001....$

These Root states must satisfy the generalized Pauli rule

Not more than one particle in 3 consecutive orbitals

(rule for 1/3 Laughlin with abelian quasiholes.)

allowed root states are “admissible” occupation configurations

- Laughlin is Abelian  $k=1$  case, Moore-Read is  $k=2$ , Read-Rezayi is general  $k$ .
- Jack parameter is  $\alpha = -(k+1)$
- Fermionic fillings  $k/(k+2)$ , Pauli rule is not more than  $k$  particles in  $(k+2)$  consecutive “orbitals”.
- $n > k$  filled-Landau level droplets are absent in the FQHE + quasihole states.  
 (fundamental fermion cluster property). This is a fundamental property of the Jack Polynomial with an “admissible” configuration and specifically chosen Jack parameter  $\alpha$  (Feigin, Jimbo, Miwa + Mukhin, 2002)



- Spectrum allows characters of cft (up to a finite-size truncation of Virasoro level) to be “read off”.
- Spectrum gives (a) conformal anomaly  $c$  (b) quantum dimensions of each sector, etc.

# The generalized Pauli rule generates the spectrum of the edge conformal field theory:

- Laughlin 1/3 vacuum with edge

$$\dots 1001001001001001001000000000 \dots \} \Delta L^z = 0 \quad (1)$$

$$\dots 1001001001001000 \overset{\bullet}{0} 10000000 \dots \} \Delta L^z = 1 \quad (1)$$

$$\dots 1001001001001000 \overset{\bullet}{0} \overset{\bullet}{0} 0100000 \dots \} \Delta L^z = 2 \quad (2)$$

$$\dots 1001001001000 \overset{\bullet}{0} 1001000000 \dots \} \Delta L^z = 2 \quad (2)$$

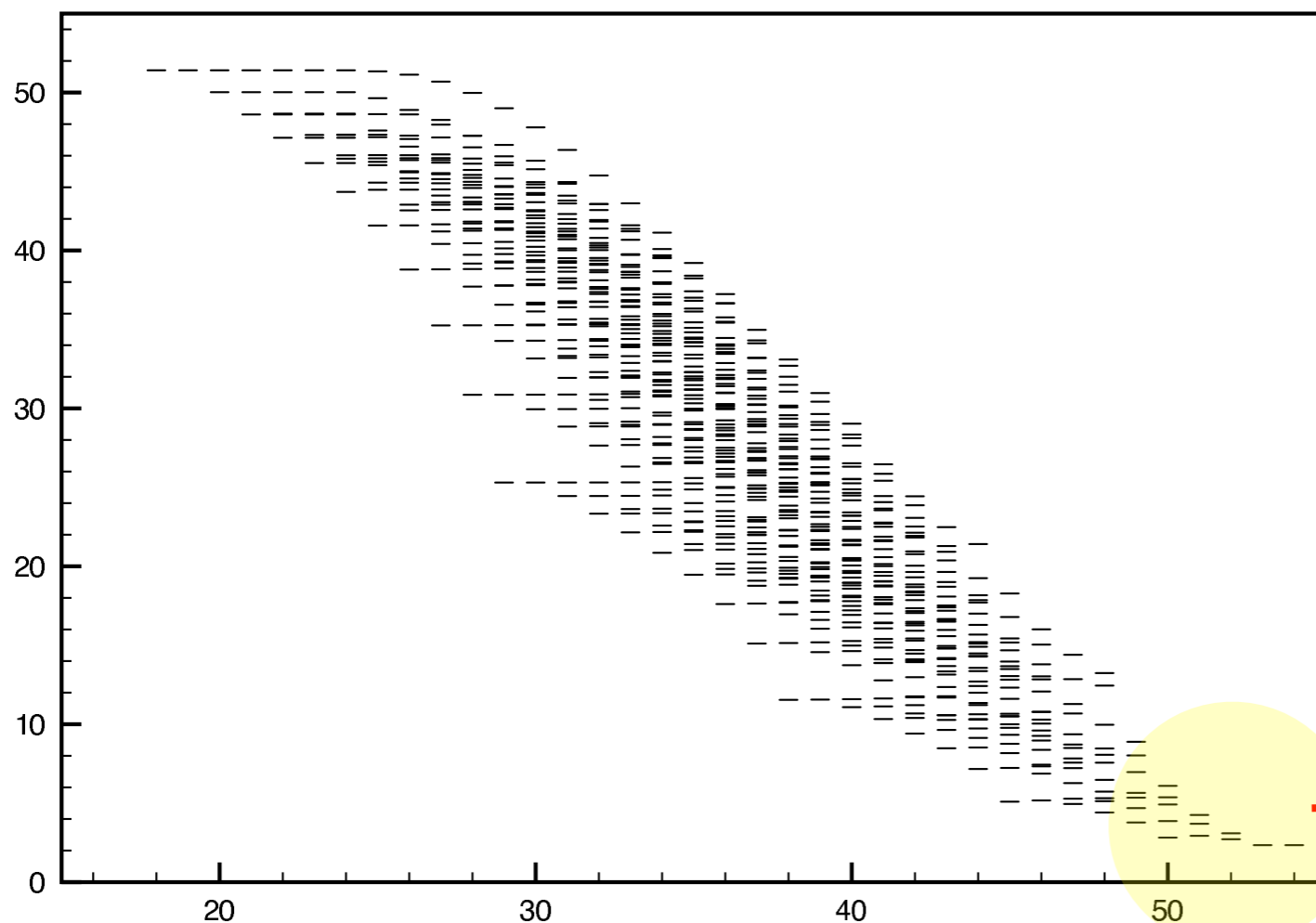
$$\dots 1001001001001000 \overset{\bullet}{0} \overset{\bullet}{0} \overset{\bullet}{0} 0010000 \dots \} \Delta L^z = 3 \quad (3)$$

$$\dots 1001001001000 \overset{\bullet}{0} 100 \overset{\bullet}{0} 0100000 \dots \} \Delta L^z = 3 \quad (3)$$

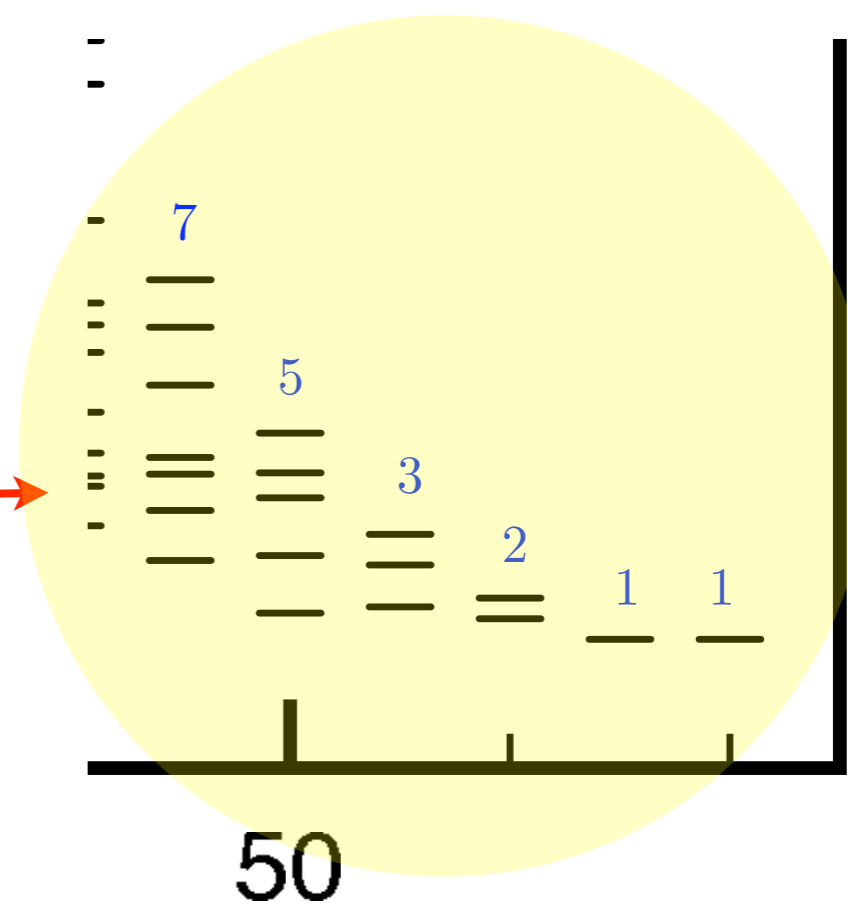
$$\dots 1001001000 \overset{\bullet}{0} 10010010000000 \dots \} \Delta L^z = 3 \quad (3)$$

(etc.)  $\Delta L^z = 4 \quad (5)$

Note: these represent Jack root configurations, the full states contain “squeezed” Slater determinant configurations completely squeezed back into the yellow region



(b)  $N = 12, N_\phi = 33$



Characters of cft (state count vs virasoro level) are reproduced  
 (up to ultra-violet cutoff from finite size of sphere)

# Interpolation between 1/3 Laughlin state and “true” ground state of Coulomb interaction.

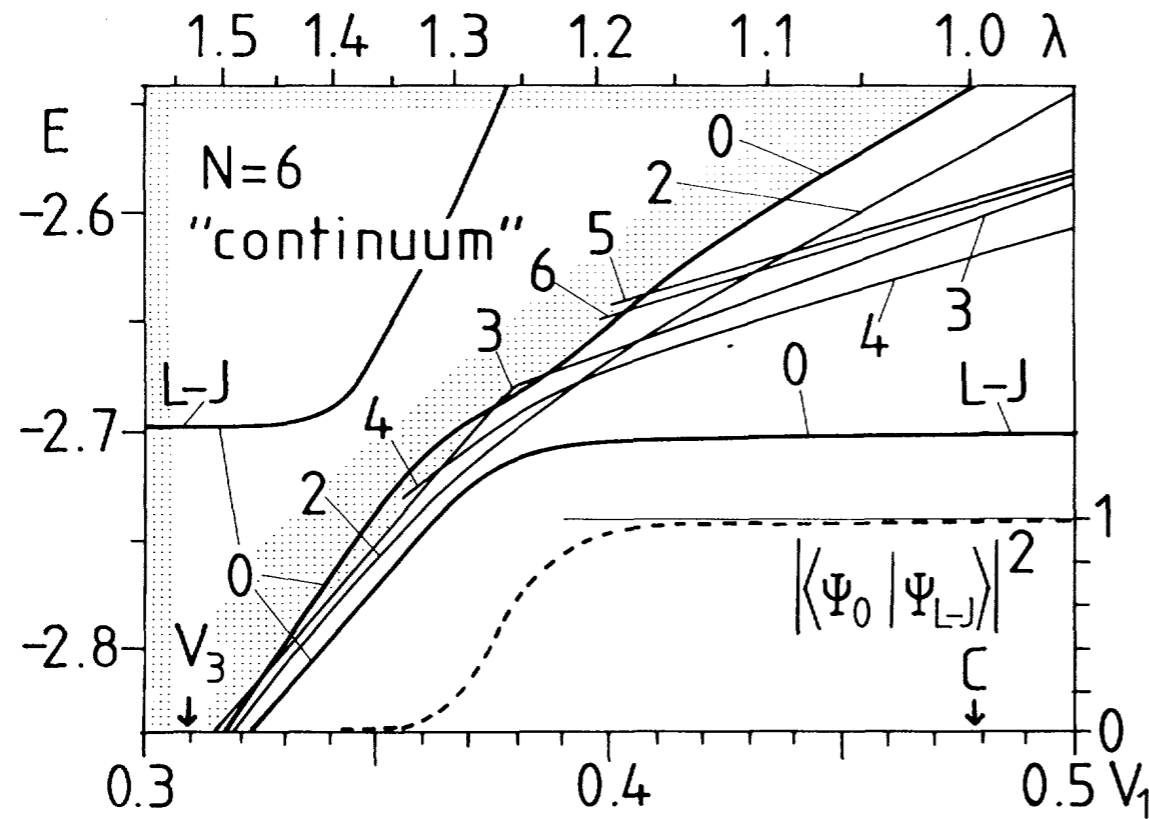


FIG. 6. Low-lying states at  $N=6$ ,  $2S=15$  ( $\nu = \frac{1}{3}$ ) as the “hard-core” pseudopotential component  $V_1$  is varied. The other  $V_m$  take their Coulomb values.  $V_3$  and the Coulomb value ( $C$ ) of  $V_1$  are marked. Angular momentum quantum numbers  $L$  are indicated. Also shown is the projection of the LJ state on the ground state. In the gapless regime ( $\lambda > 1.25$ ), the LJ state reappears as the *highest*  $L=0$  level.

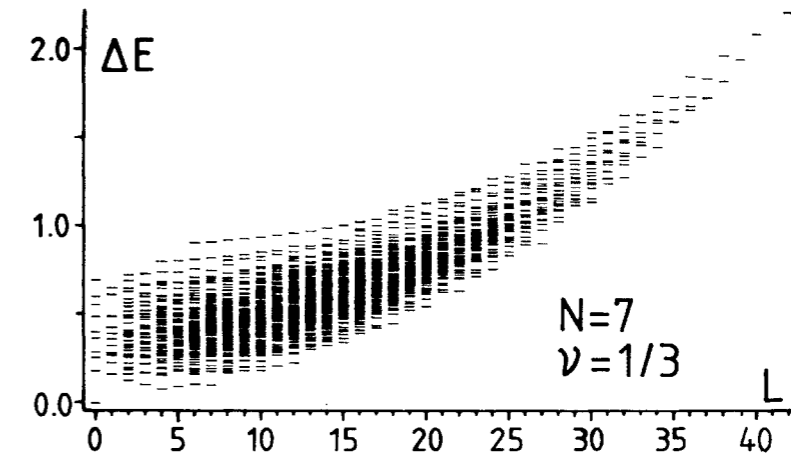


FIG. 1. The spectrum of 1656 multiplets (50388 states) of the  $N=7$  electron,  $2S=18$  flux quanta system with Coulomb interactions, grouped by total angular momentum  $L$ . Energies (in units of  $e^2/4\pi\epsilon l$ ) are shown relative to the incompressible ( $\nu = \frac{1}{3}$ ) isotropic ( $L=0$ ) ground state.

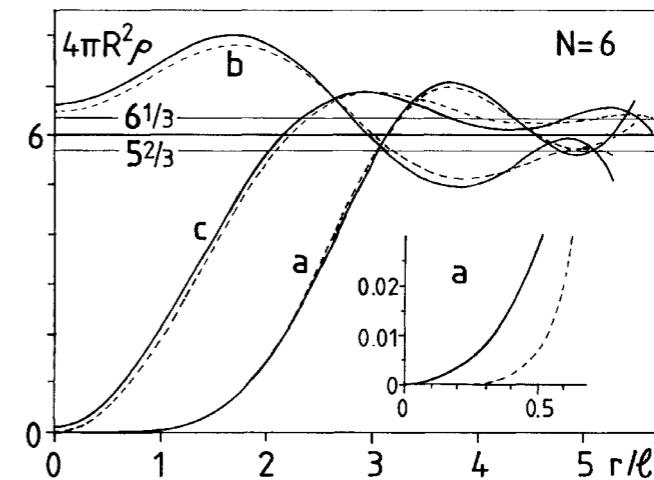


FIG. 3. (a) Ground-state pair correlation function for  $\nu = \frac{1}{3}$ ,  $N=6$ . (b), (c) Density profiles of localized quasiparticle and quasihole defects. The condensate density  $\rho$  satisfies  $4\pi R^2 \rho = 6$ ,  $5\frac{2}{3}$ , and  $6\frac{1}{3}$ , respectively. Filled curves, Coulomb interaction; broken curves, model Laughlin-Jastrow wave functions.

Look at difference between Laughlin state, entanglement spectrum and state that interpolates to Coulomb ground state.

3

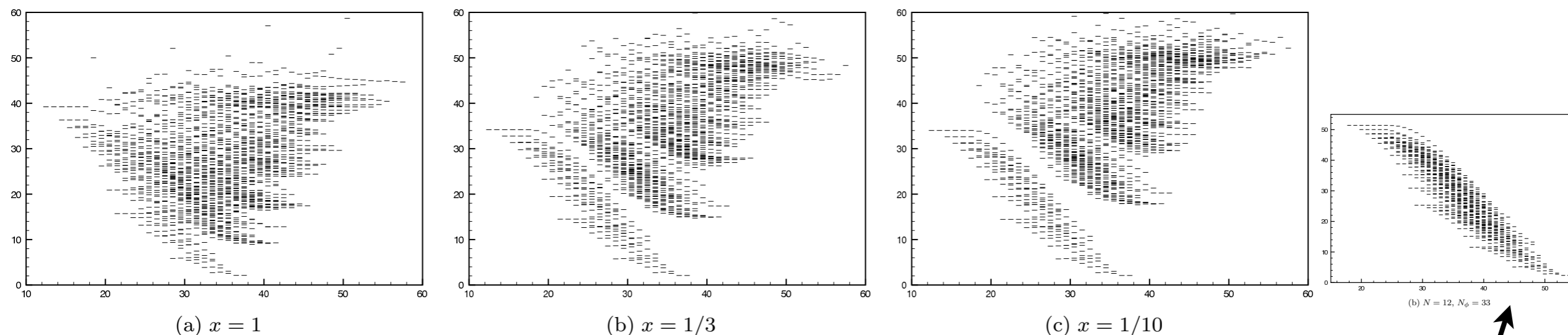


FIG. 2: Entanglement spectrum for the ground state, for a system of  $N = 10$  electrons in the lowest Landau level on a sphere enclosing  $N_\phi = 27$  flux quanta, of the Hamiltonian in Eq. (12) for various values of  $x$ .

$$H = xH_c + (1 - x)V_1$$

**x=0 is pure  
Laughlin**

Can we identify topological order in “physical as opposed to model wavefunctions from low-energy entanglement spectra?”

- Moore-Read  $5/2 = (2+) 2/4$ :

... 1100110011001100110000000000 ...

ground state of a boundary of a droplet containing an even number of  $-e/4$  quasiholes

... 1010101010101010100000000000 ...

ground state of a boundary of a droplet containing an odd number of  $-e/4$  quasiholes

# Similar calculations for Moore-Read state

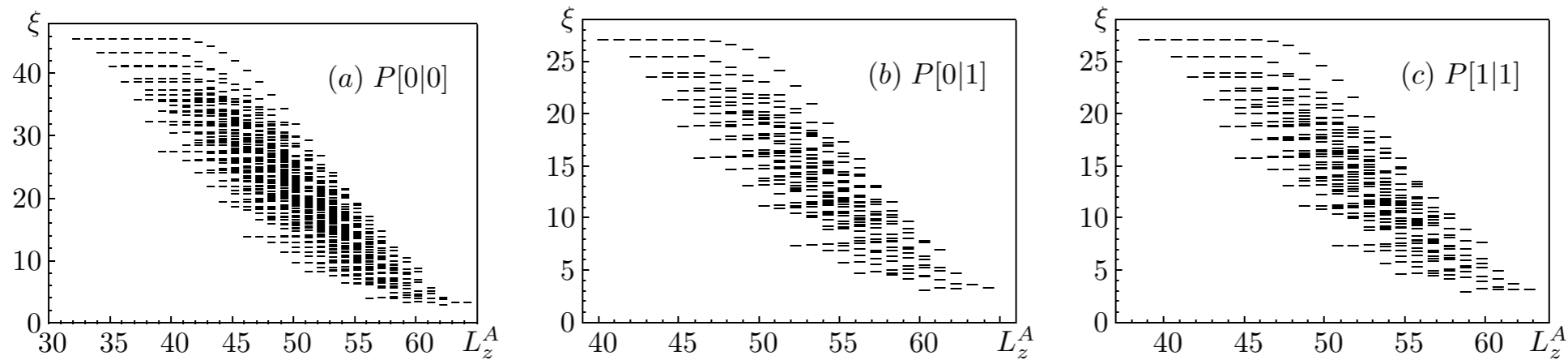


FIG. 1: The complete entanglement spectra of the  $N_e = 16$  and  $N_{orb} = 30$  Moore-Read state (only the relative values of  $\xi$  and  $L_z^A$  are meaningful).

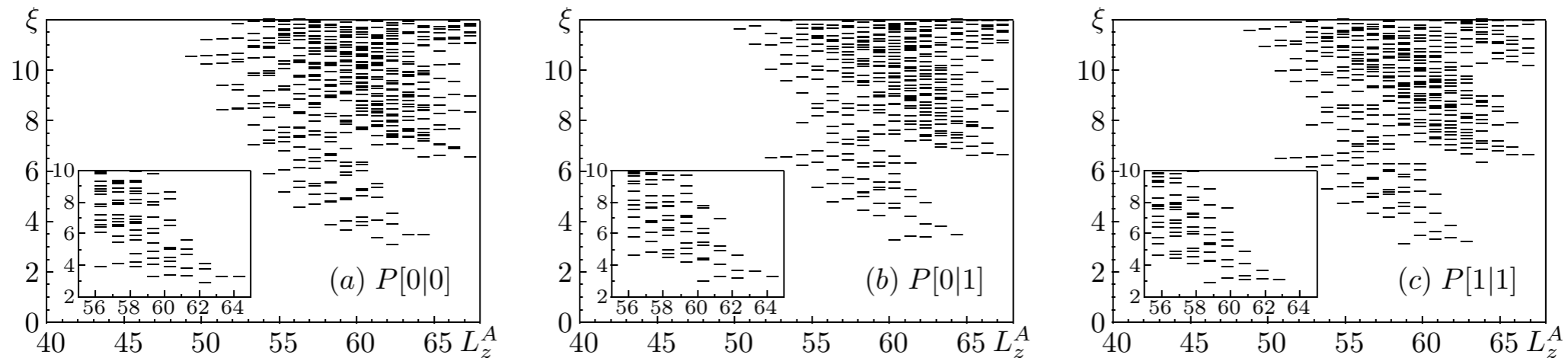


FIG. 2: The low-lying entanglement spectra of the  $N_e = 16$  and  $N_{orb} = 30$  ground state of the Coulomb interaction projected into the second Landau level (there are levels beyond the regions shown here, but they are not of interest to us). The insets show the low-lying parts of the spectra of the Moore-Read state, for comparison [see Figure (1)]. Note that the structure of the low-lying spectrum is essentially identical to that of the ideal Moore-Read state.

# Gap to non-cft entanglement levels states of “generic” states appear to remain finite in the thermodynamic limit.

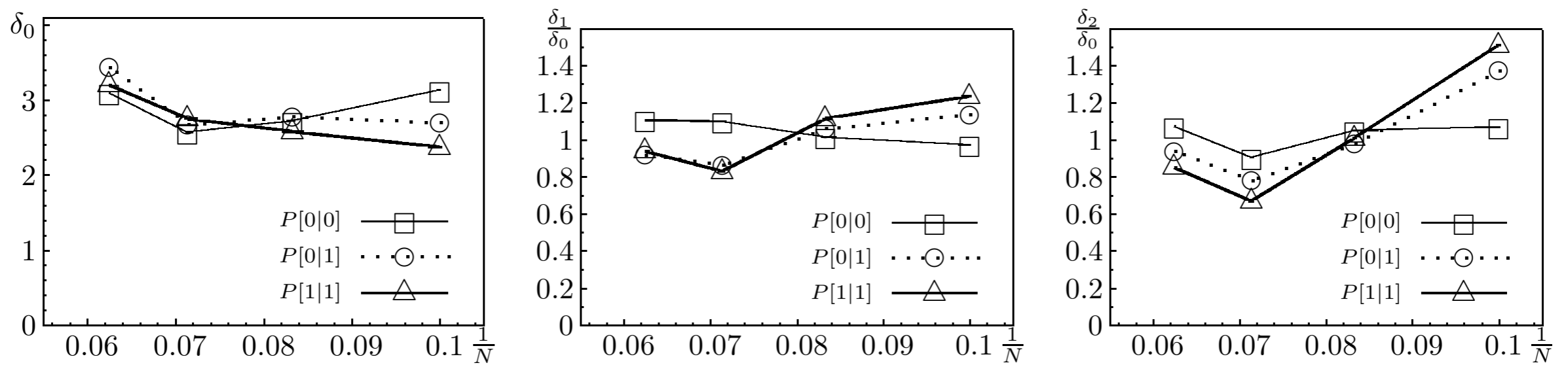


FIG. 3: Entanglement gap as a function of  $1/N$ .  $\delta_0$  is the gap at  $\Delta L = 0$ , i.e., the distance from the single CFT level at  $\Delta L = 0$  to the bottom of the generic (non-CFT) levels at  $\Delta L = 0$ . At  $\Delta L = 1, 2$ , the gap  $\delta_{1,2}$  is defined as the distance from the average of the CFT levels to the bottom of the generic levels. See Table I for the details of various partitionings.



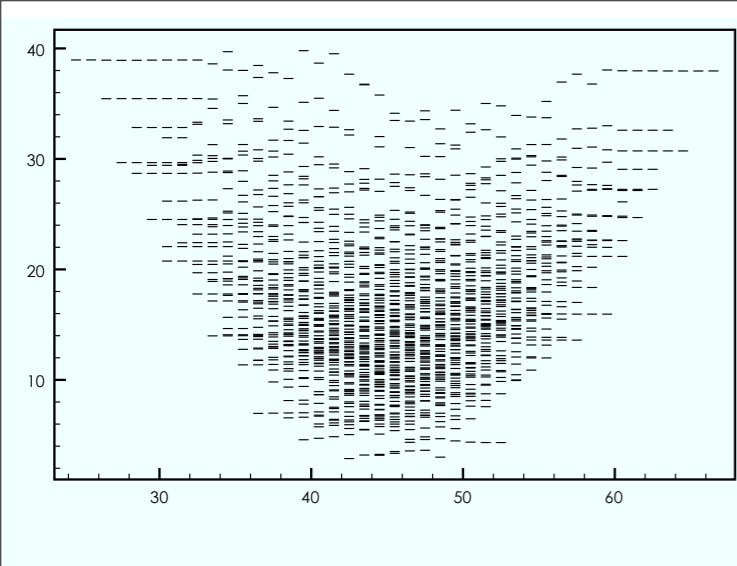


FIG. 1:  $\delta V_1 = -0.05$

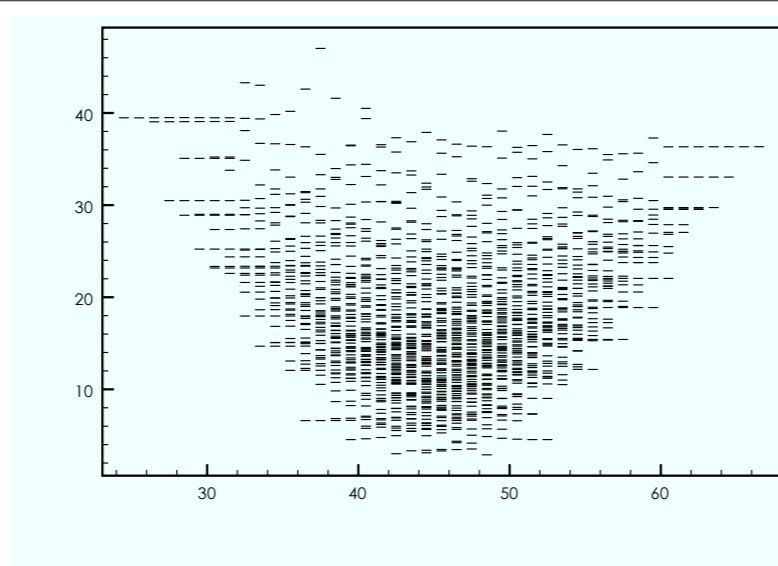


FIG. 2:  $\delta V_1 = -0.02$

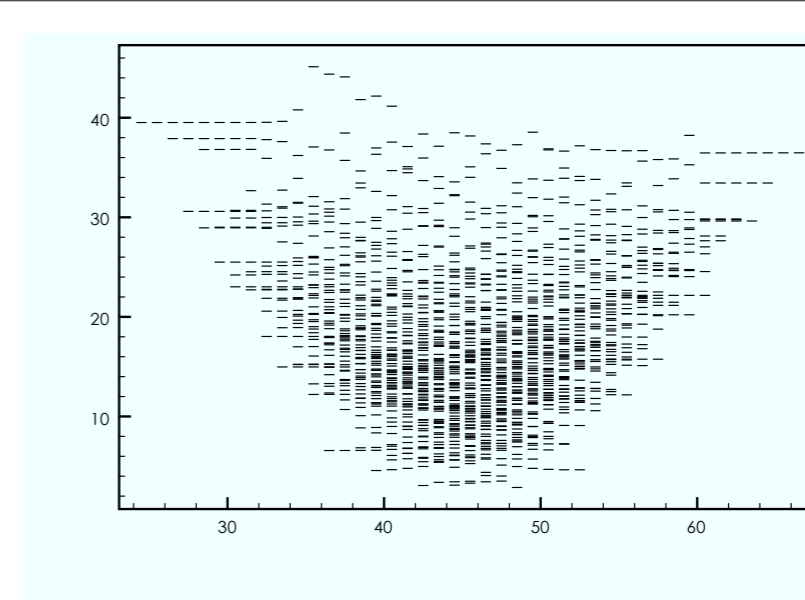


FIG. 3:  $\delta V_1 = -0.015$

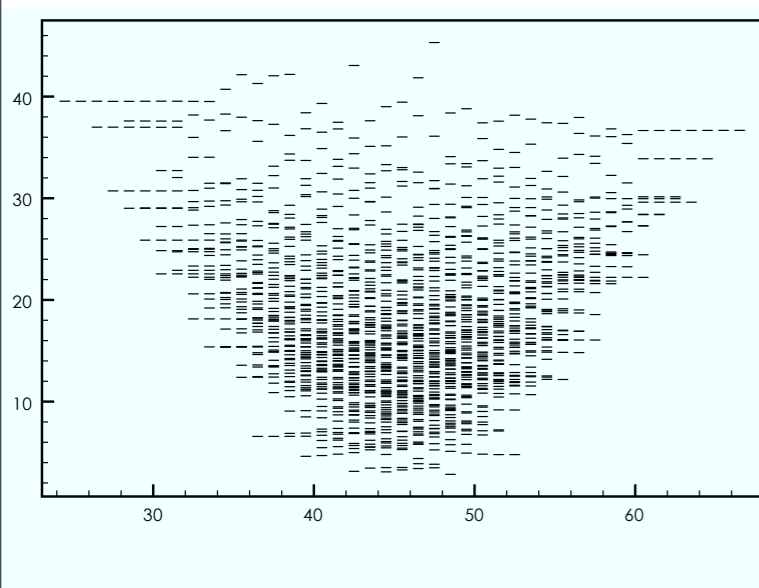


FIG. 4:  $\delta V_1 = -0.01$

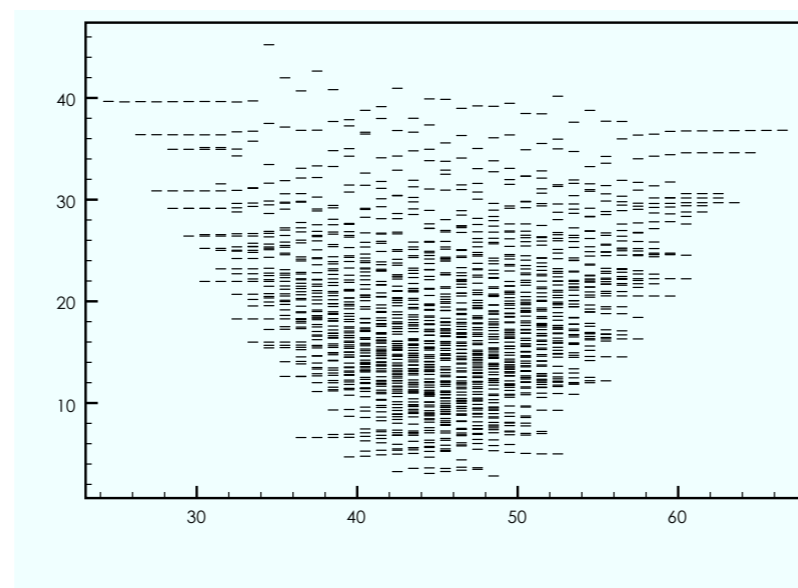


FIG. 5:  $\delta V_1 = -0.005$

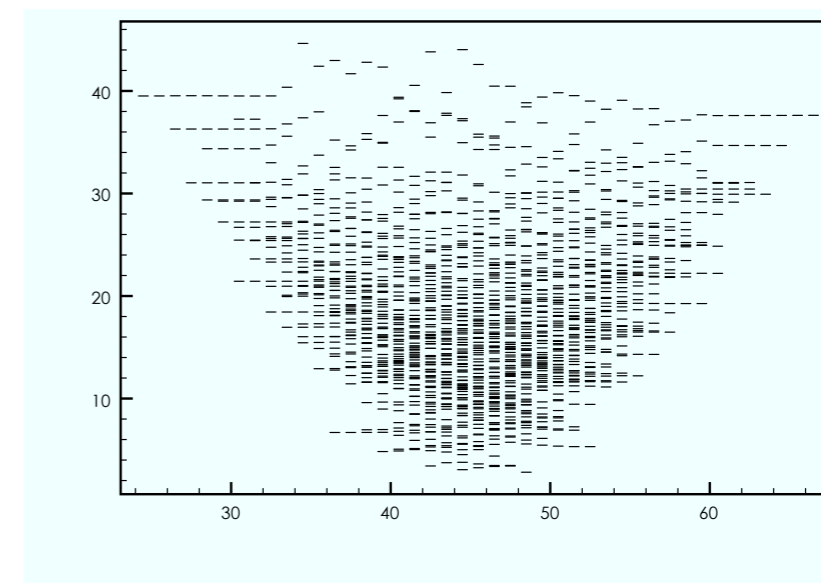


FIG. 6:  $\delta V_1 = 0$

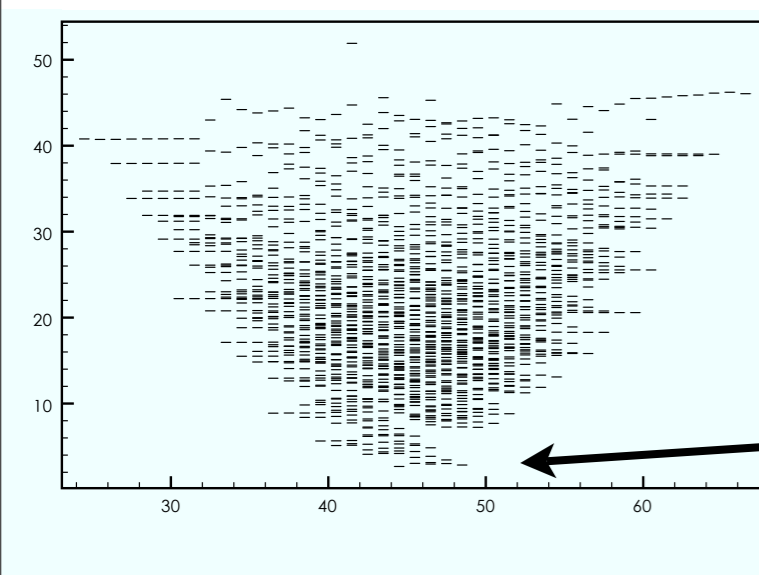


FIG. 7:  $\delta V_1 = 0.04$

low-lying entanglement spectrum  
matches that of pure MR state



# “Entanglement spectrum” (free fermions)

- Divide infinite crystal along a lattice plane into two semi-infinite regions
- can find a unitary change of basis of occupied states where

$$|\Psi\rangle = \prod_{\alpha, \mathbf{k}_\perp} \left( u_{\alpha \mathbf{k}_\perp} c_{\alpha \mathbf{k}_\perp L}^\dagger + v_{\alpha \mathbf{k}_\perp} c_{\alpha \mathbf{k}_\perp R}^\dagger \right) |\text{vac}\rangle$$

$|u_{\alpha \mathbf{k}_\perp}|^2 + |v_{\alpha \mathbf{k}_\perp}|^2 = 1$

- Density matrix spectrum

$$\hat{\rho}_L \propto e^{-\hat{\mathcal{E}}_L} \quad \hat{\rho}_R \propto e^{-\hat{\mathcal{E}}_R}$$

- “Entanglement spectrum”:

$$\hat{\mathcal{E}} = \sum_{\alpha \mathbf{k}_\perp} \varepsilon_{\alpha \mathbf{k}_\perp} n_{\alpha \mathbf{k}_\perp}$$

$$\varepsilon_{\alpha \mathbf{k}_\perp R} = \log \left( \frac{|u_{\alpha \mathbf{k}_\perp}|^2}{|v_{\alpha \mathbf{k}_\perp}|^2} \right)$$

$$n_{\alpha \mathbf{k}_\perp} = 0, 1$$

cut

Left

$P_L$

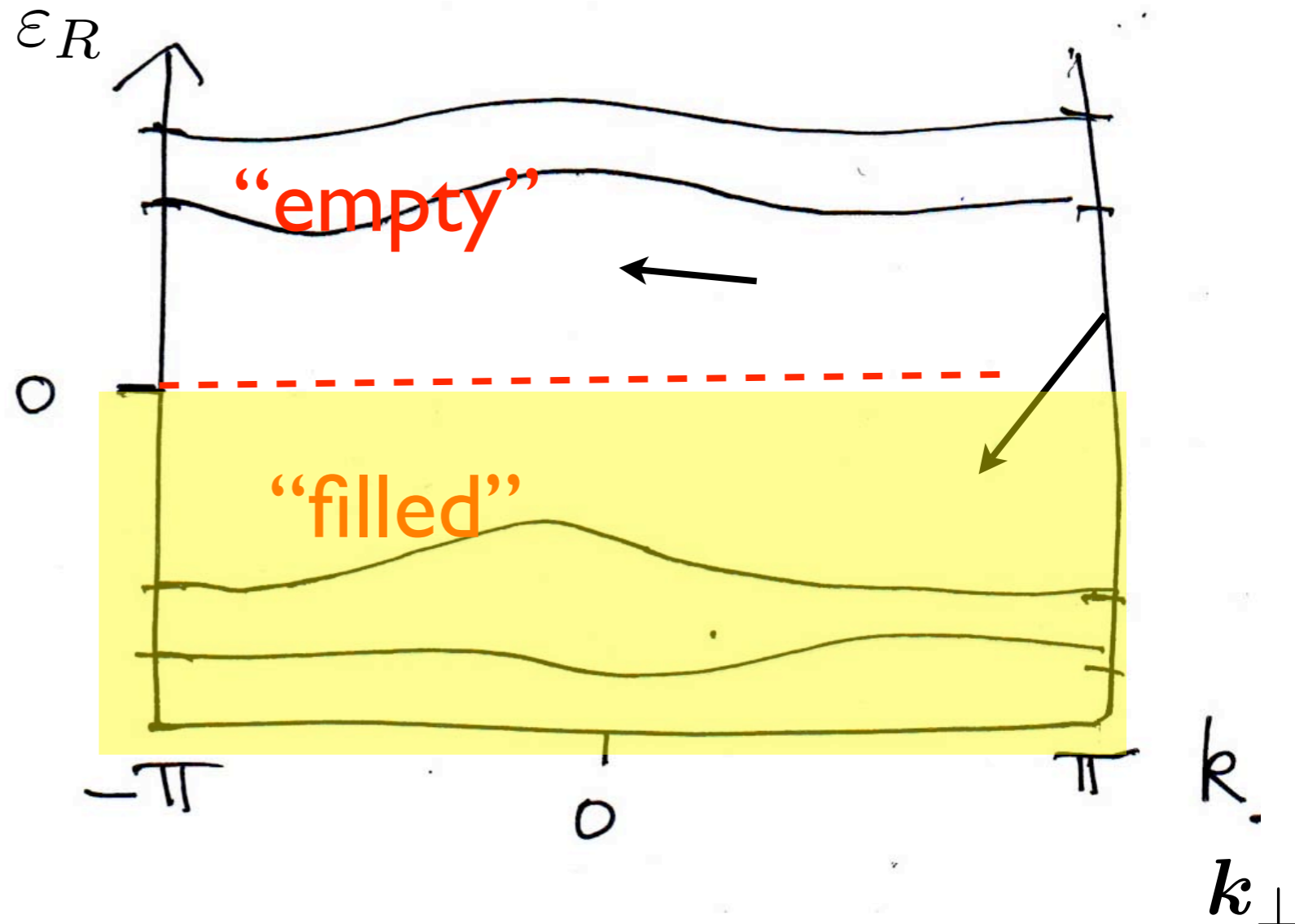
Right

$P_R$

Bloch vector parallel to “cut”

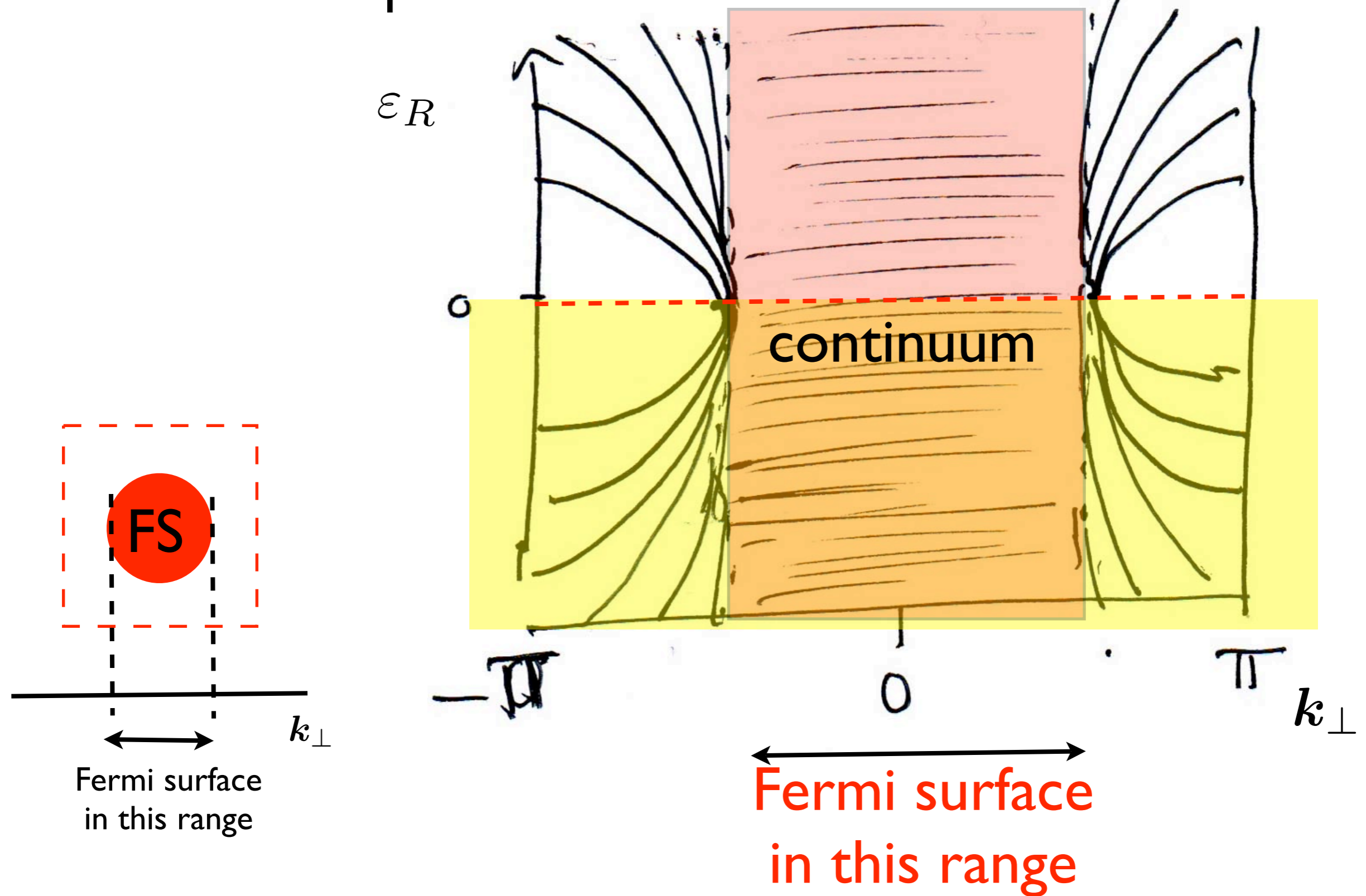
# generic “entanglement spectrum” of a band insulator

- levels below 0 occupied in “ground state” (dominant term in (Schmidt) expansion)
- varies as lattice plane of cut is moved: bands move from empty to filled region (spectral flow)



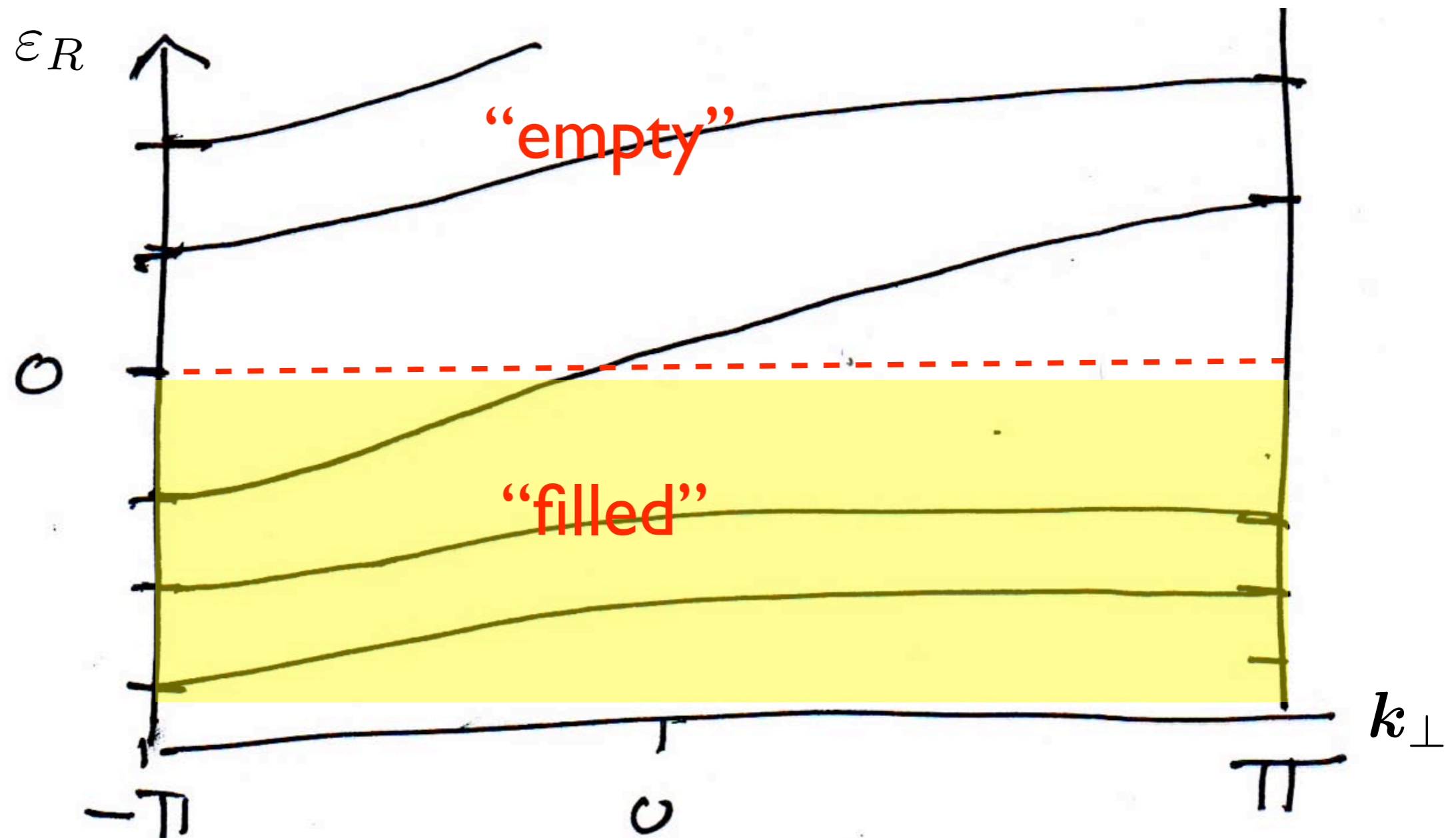
(quite different if a Fermi surface is present)

# spectrum with a Fermi surface



levels coalesce into a continuum if a Fermi surface is present  
(density of states proportional to  $\log(\text{width})$  for a finite width (not semi-infinite) region.)

# topologically-non-trivial “band insulator”



- topologically-non-trivial filled bands show “spectral flow” as a function of  $k_{\perp}$

# 2D zero-field Quantized Hall Effect

FDMH, Phys. Rev. Lett. 61, 2015 (1988).

- 2D quantized Hall effect:  $\sigma^{xy} = \nu e^2/h$ . In the absence of interactions between the particles,  $\nu$  must be an integer. There are no current-carrying states at the Fermi level in the interior of a QHE system (all such states are localized on its edge).
- The 2D integer QHE does NOT require Landau levels, and can occur if time-reversal symmetry is broken even if there is no net magnetic flux through the unit cell of a periodic system. (This was first demonstrated in an explicit “graphene” model shown at the right.)
- Electronic states are “simple” Bloch states! (real first-neighbor hopping  $t_1$ , complex second-neighbor hopping  $t_2 e^{i\phi}$ , alternating onsite potential  $M$ .)

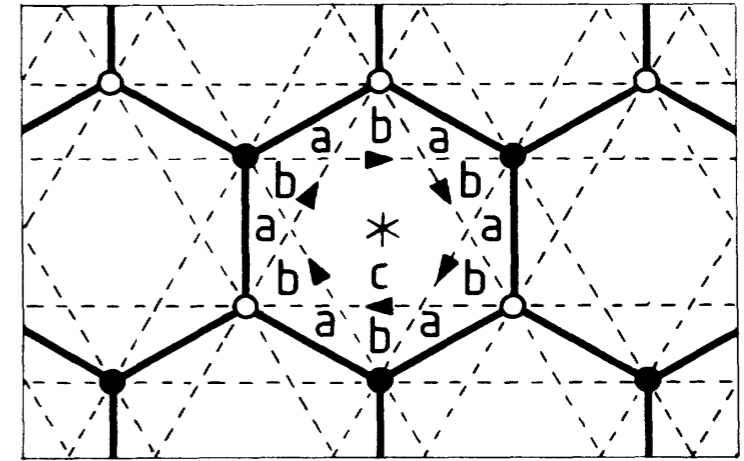


FIG. 1. The honeycomb-net model (“2D graphite”) showing nearest-neighbor bonds (solid lines) and second-neighbor bonds (dashed lines). Open and solid points, respectively, mark the  $A$  and  $B$  sublattice sites. The Wigner-Seitz unit cell is conveniently centered on the point of sixfold rotation symmetry (marked “\*”) and is then bounded by the hexagon of nearest-neighbor bonds. Arrows on second-neighbor bonds mark the directions of positive phase hopping in the state with broken time-reversal invariance.

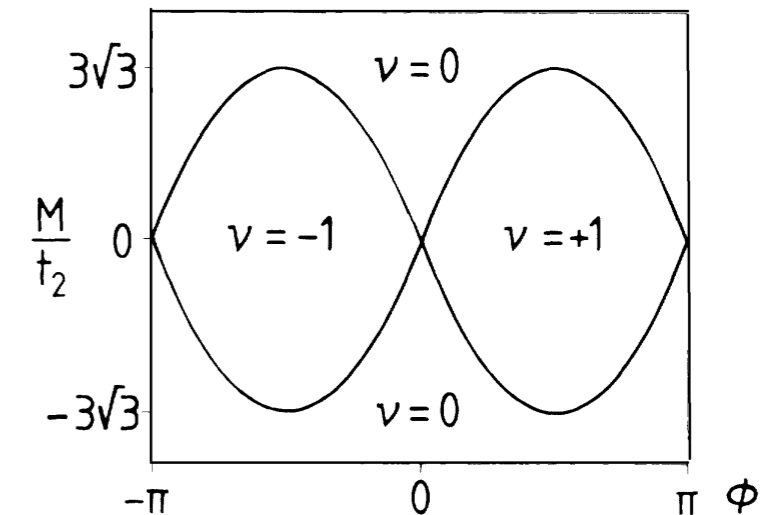
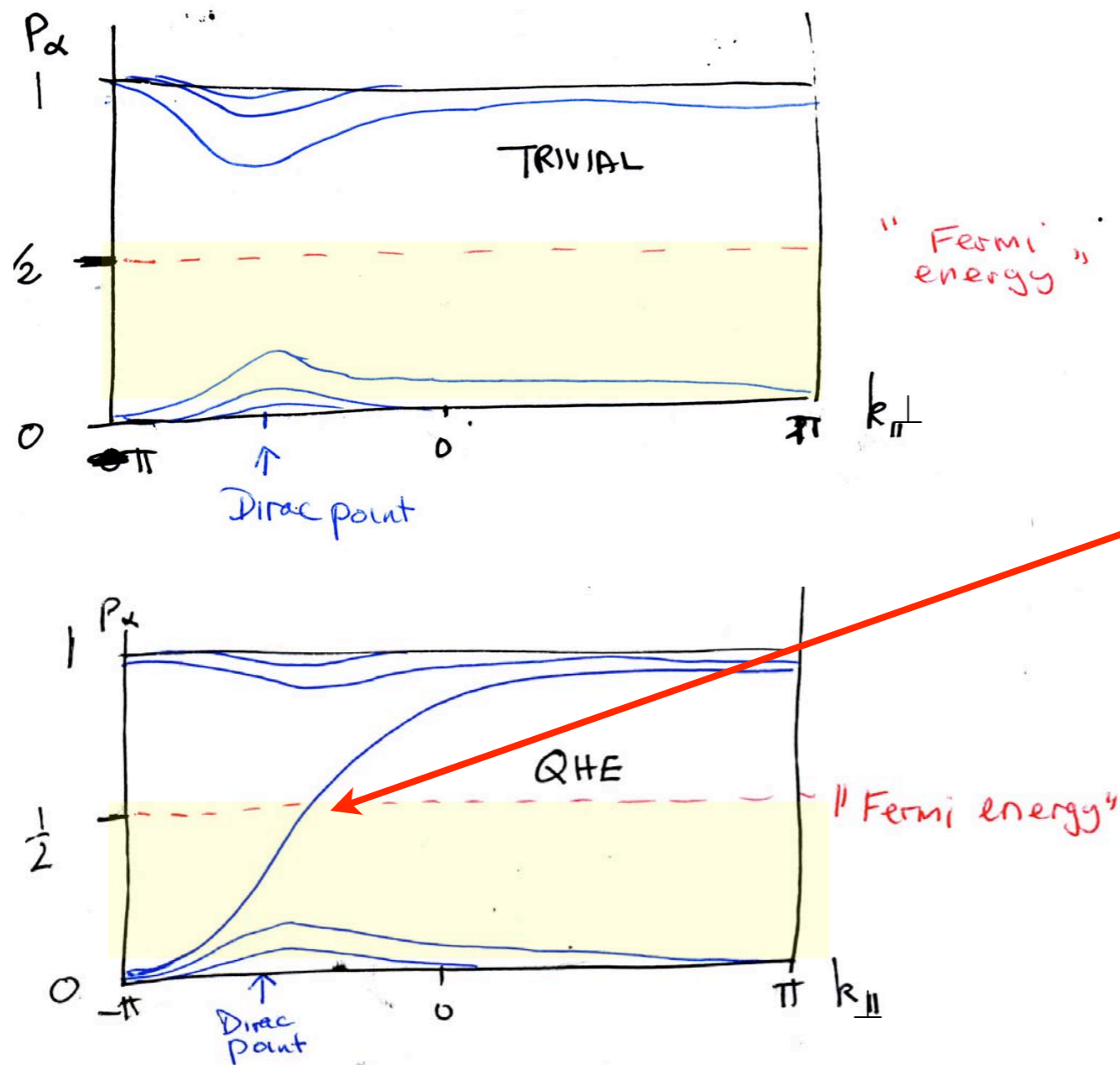


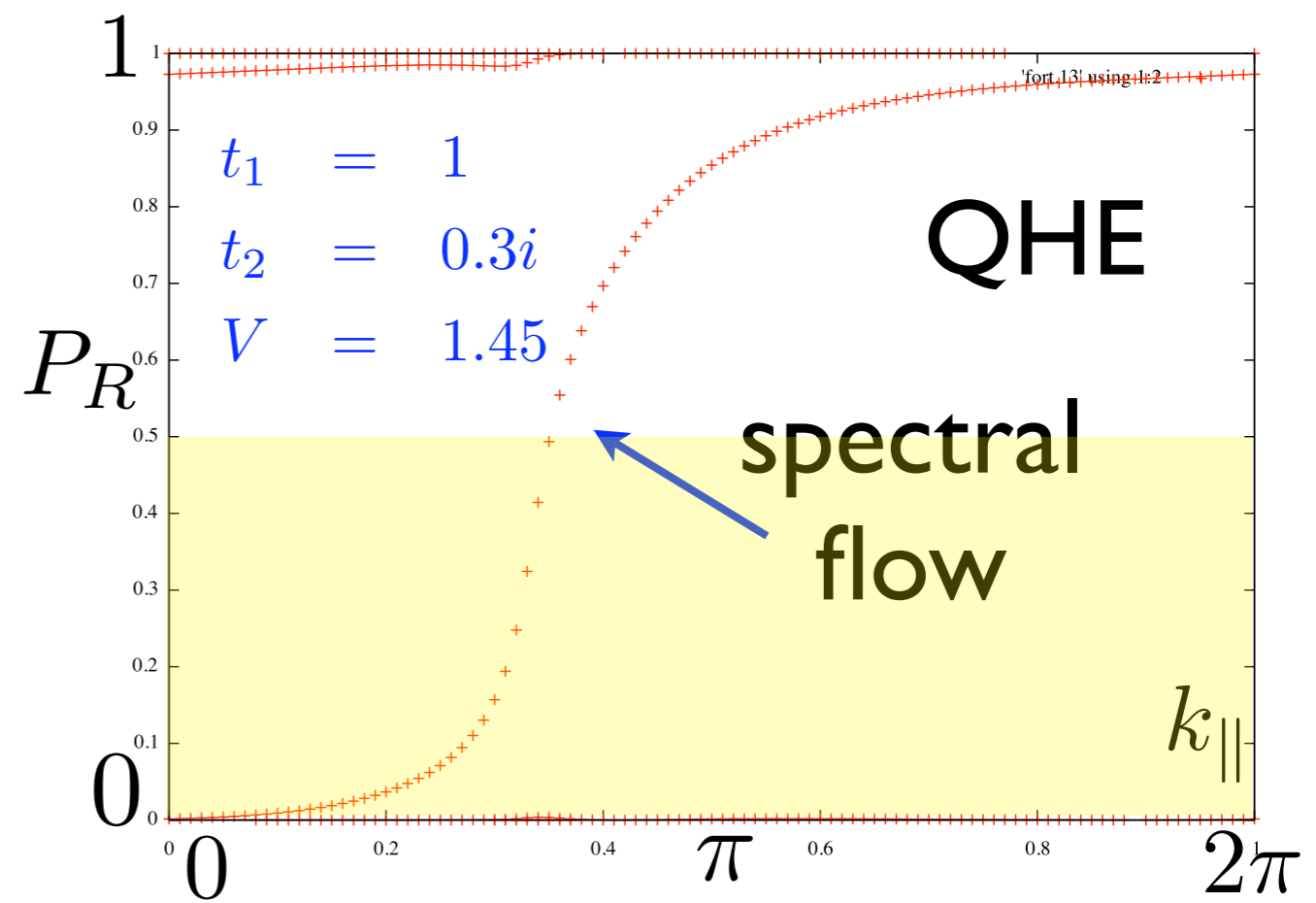
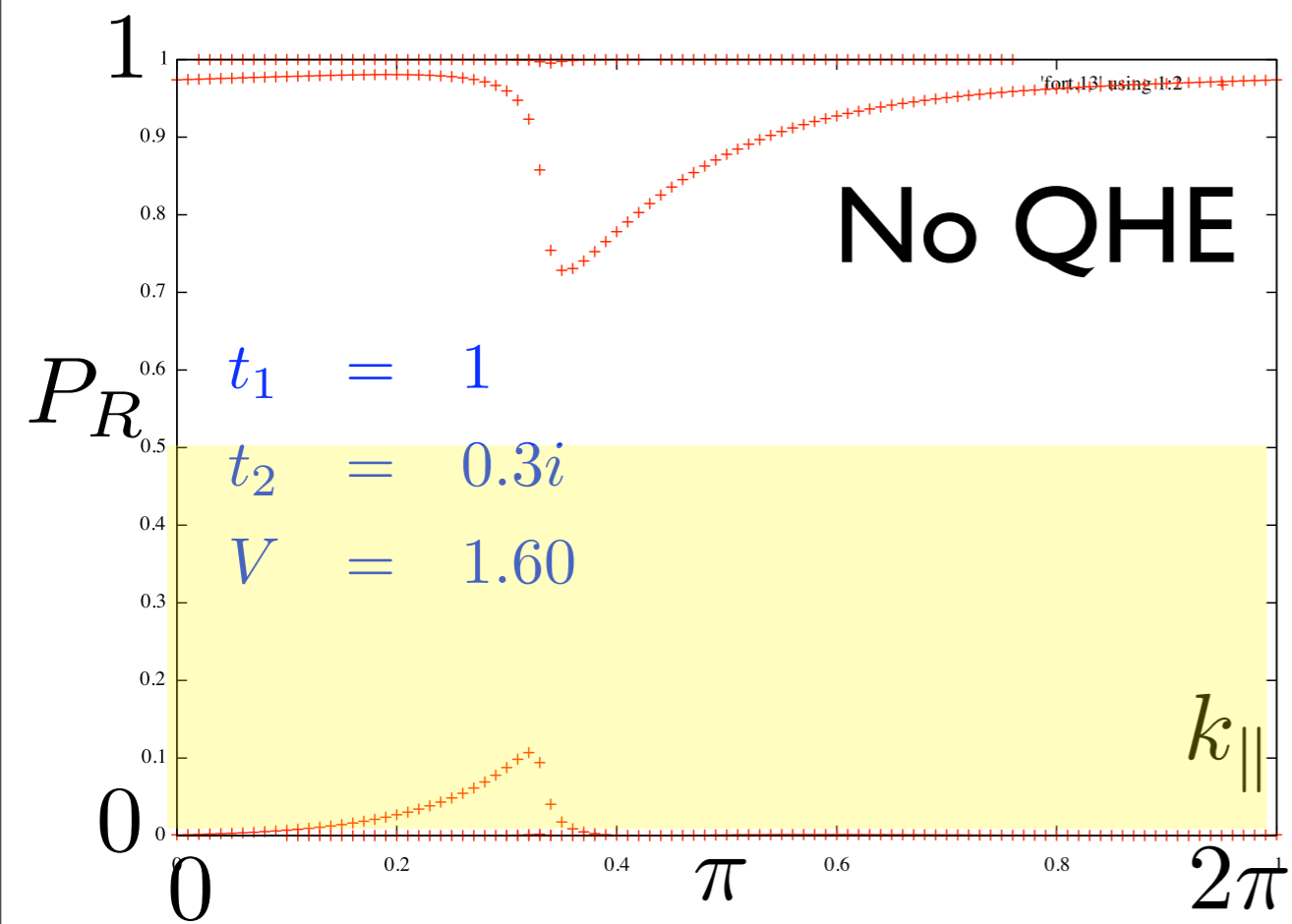
FIG. 2. Phase diagram of the spinless electron model with  $|t_2/t_1| < \frac{1}{3}$ . Zero-field quantum Hall effect phases ( $\nu = \pm 1$ , where  $\sigma^{xy} = \nu e^2/h$ ) occur if  $|M/t_2| < 3\sqrt{3}|\sin\phi|$ . This figure assumes that  $t_2$  is positive; if it is negative,  $\nu$  changes sign. At the phase boundaries separating the anomalous and normal ( $\nu=0$ ) semiconductor phases, the low-energy excitations of the model simulate undoubled massless chiral relativistic fermions.

single-particle entanglement spectrum (schematic, but confirmed by actual calculations, WIP) (Zig-zag cut)



generates free fermion cft ( $c=1$ ) as full entanglement spectrum.

“spectral flow” from L to R as  $k_{\perp}$  changes



$t_1 = 1$   
 $t_2 = 0.3i$   
 $V_c = 1.55$

entanglement  
 spectrum across  
 “zigzag” cut  
 (“graphene” with T and I breaking)



- Gapless nature of “entanglement spectrum” seems quite universal in topological order
- Simple “ideal states” have less quantum fluctuations than generic ones, have **ONLY** the (required) spectrum of the topological order.
- spectrum seems to be a more useful characterization of entanglement than “just” a single number, the Von Neumann entropy.